

Assessment of post-liquefaction potential in soil displacement on irrigation canal reconstruction project in the Jono Oge and Lolu area, Central Sulawesi, Indonesia

I Made Widyanata^{1,2}, Sito Ismanti^{1*}, and Angga Fajar Setiawan¹

¹Department of Civil and Environment Engineering, Faculty of Engineering, Universitas Gadjah Mada, Yogyakarta 55281, Indonesia

²Directorate General of Construction Development, The Ministry of Public Works and Housing, South Jakarta 12110, Indonesia

Abstract. A seismic event of magnitude 7.5 Mw took place in Central Sulawesi in September 2018, marking a significant occurrence in the geological hazard chronicles of Indonesia. The occurrence of liquefaction subsequent to the earthquake significantly damaged the water resource infrastructure in the Sigi Regency. This study aims to evaluate the possible soil displacement resulting from re-liquefaction events occurring in the main irrigation canals in the Jono Oge and Lolu regions. The study used semi-empirical and finite element analysis to compute the lateral displacement index and reconsolidation settlement within the designated study region. The examination of soil displacement is conducted under various groundwater level scenarios, utilizing the most recent soil investigation conducted in 2021. The findings of the study indicate that raising the groundwater level to -3.5 meters will result in significant soil and irrigation canal damage. In the future, it is suggested that limiting the groundwater level below -11 meters in the primary irrigation canal area might effectively mitigate soil lateral displacement and settlement.

1 Introduction

The Sigi Regency in Central Sulawesi saw a significant effect due to geo-hazard events, specifically 7.5 Mw earthquakes and liquefaction, throughout 2018. Liquefaction occurrences were observed in several localities within the Sigi Regency, including Balaroa, Petobo, Jono Oge, Lolu, and Sibalaya. As documented in previous studies, the regions mentioned above-encountered ground lateral spreading and flow-slide liquefaction [1,2]. The government must address the necessary repairs to the infrastructure, including the irrigation system that spans multiple villages in Sigi Regency. The primary irrigation canal structures in the Jono Oge and Lolu regions suffered significant damage, rendering them incapable of meeting the water requirements for crops. This damage was mainly attributed to soil displacement resulting from liquefaction. Figure 1 depicts the irrigation channel that has incurred damage.

The Ministry of Public Works and Housing has undertaken efforts to restore the functionality of the irrigation system in the Sigi regency. Considering potential re-liquefaction in future scenarios holds significant importance in infrastructure planning. The assessment of liquefaction's severity and potential impacts on infrastructure can be conducted by utilizing the soil Lateral Displacement Index (LDI) and reconsolidation settlement. Considering the soil LDI and the settlement is crucial when evaluating the

phenomenon of ground displacement generated by liquefaction. Previous research has investigated the extent of the soil lateral displacement and settlement in the Jono Oge and Paneki river regions [3,4]. Nevertheless, a comprehensive investigation into the precise assessment of soil displacement in the irrigation canals of Jono Oge and Lolu has not been conducted thus far. Additional research is necessary to evaluate the potential occurrence of soil displacement, as indicated by recent soil investigations conducted at the reconstruction site.



Fig. 1. The extensive damage in the Jono Oge irrigation canal.

This study aims to assess the potential soil displacement and the extent of damage that could arise along the irrigation canal in the event of future re-liquefaction. The soil lateral displacement and settlement were calculated using the [5] and [6] equations, which is a semi-empirical analysis method. In addition, a finite element analysis was conducted to

*Corresponding author: sito.ismanti@ugm.ac.id

assess the soil displacement, considering dynamic loading conditions. The analysis uses soil data from the Standard Penetration Test (SPT) conducted at thirteen locations along the irrigation restoration project site in the Jono Oge and Lolu area. This study primarily aims to examine the potential implications of re-liquefaction on Sigi Regency, explicitly focusing on local engineers.

2 Theory and background

The geological conditions play a substantial role in the phenomenon of soil liquefaction. According to the geological condition map, it can be observed that the Sigi Regency is predominantly composed of the Pakuli Formation, which is characterized by its deposition of alluvium and coastal sediments [7]. The sediment in concern is classified as new deposits/quaternary sediment. In general, recently deposited soils exhibit a higher susceptibility to liquefaction than soils that have been in place for a more extended period. It is of utmost importance to comprehend the geological conditions and their impact on soil liquefaction to evaluate an area's susceptibility and develop suitable measures for mitigating the potential harm caused by liquefaction [8].

The presence of saturated sandy soils characterized by loose to medium density, shallow groundwater levels, and varying soil compositions, including clay, silty, and sandy soil, can enhance the vulnerability of the soil to liquefaction in the event of seismic activity [9,10]. Figure 2 illustrates that the soil strata along Jono Oge and Lolu's primary canal consist predominantly of sand.



Fig. 2. The presence of sandy soil along the study area.

The September 28, 2018, seismic event substantially influenced the Sigi Regency's geological state, especially in the Jono Oge village. The occurrence of liquefaction and flow-slide over the relatively flat terrain of Jono Oge was a direct consequence of the earthquake [11]. The village of Jono Oge, situated in the Palu basin, exhibited the highest degree of land displacement compared to other regions [12]. The significant issue was the soil deformation resulting from lateral displacement in the Jono Oge and Lolu regions.

The seismic event 2018 resulted in extensive damage and horizontal displacement inside the soil structure of the irrigation canal. The acceleration of water flow in the Gumbasa Irrigation Canal resulted in deformation, ultimately causing the occurrence of mudflows via fissures in the ground [12]. The soil deformation seen in the Jono Oge region can be ascribed to shear deformation caused by the direct thrust of the soft soil and the flow thrust [13].

2.1 Lateral displacement Index (LDI)

The lateral displacement index is a quantitative measure employed to assess the likelihood of soil lateral displacements that may occur due to ground movements induced by liquefaction during significant seismic events [5]. The derivation involves the integration of the maximum cyclic shear strains as a function of depth. The determination of the Lateral Displacement Index (LDI) involves the integration of data obtained from the Standard Penetration Test (SPT) or Cone Penetration Test (CPT), along with laboratory test results of the maximum shear strain shown by saturated soils. The LDI offers an initial assessment of the extent of horizontal movements caused by lateral spread triggered by liquefaction [5]. The equation used to determine the LDI value's magnitude is 1-9.

$$LDI = \int_0^{z_{max}} \gamma_{max} dz \quad (1)$$

$$\gamma_{max} = \min \left(\gamma_{lim}, 0.035(2 - FS_{liq}) \left(\frac{1 - F_{\alpha}}{FS_{liq} - F_{\alpha}} \right) \right) \quad (2)$$

$$\gamma_{lim} = 1.859 \left(1.1 - \sqrt{\frac{(N_1)_{60cs}}{46}} \right) \geq 0 \quad (3)$$

$$F_{\alpha} = 0.032 + 0.69\sqrt{(N_1)_{60cs}} - 0.13(N_1)_{60cs} \quad (4)$$

$$(N_1)_{60cs} = (N_1)_{60} + \Delta(N_1)_{60} \quad (5)$$

$$(N_1)_{60} = C_N N_{60} \quad (6)$$

$$C_N = \left(\frac{P_a}{\sigma'_{v'}} \right)^m \leq 1.7 \quad (7)$$

$$m = 0.784 - 0.0768(\sqrt{(N_1)_{60cs}}) \quad (8)$$

$$\Delta(N_1)_{60} = \exp \left(1.63 - \frac{9.7}{FC + 0.01} - \left(\frac{15.7}{FC + 0.01} \right)^2 \right) \quad (9)$$

In which in (1) z_{max} is the maximum depth, γ_{max} is the maximum shear strain, and dz is the layer thickness. The 2nd equation is applied if $2 > FS_{liq} > F_{\alpha}$ due to $FS_{liq} > 2$ and then $\gamma_{max} = 0$. Also, for equation (4), $\gamma_{max} = \gamma_{lim}$ if $FS_{liq} \leq F_{\alpha}$, where γ_{lim} is known as limiting shear strain, F_{α} is an additional parameter safety factor, FS_{liq} is the factor of safety of liquefaction initiation, and $(N_1)_{60cs}$ is penetration resistance in clean sand. A considerable quantity of lateral spreading adds to each layer spreading in meters.

2.1.1 The safety factor of liquefaction (FS_{liq})

The factor of safety (FS_{liq}) for liquefaction assesses the ability of soil to withstand liquefaction induced by seismic forces. The ratio being referred to is the relationship between the cyclic resistance ratio (CRR) and the cyclic shear stress ratio (CSR). FS_{liq} is calculated using equation 10, as outlined in the simplified procedure proposed by [14].

$$FS_{liq} = \frac{CRR_{M,\sigma'_{v'}}}{CSR} \quad (10)$$

CRR is the required cyclic shear stress for liquefaction, as calculated by Equations 11-16.

$$CRR_{M,\sigma'_{v'}} = CSR_{M=7.5,\sigma'_{v}=1} \cdot MSF \cdot K_{\sigma} \quad (11)$$

$$CRR_{M=7.5, \sigma'_v=1atm} = \exp\left(\frac{(N_1)_{60cs}}{14.1} + \right) \quad (12)$$

$$\left(\frac{(N_1)_{60cs}}{126}\right)^2 - \left(\frac{(N_1)_{60cs}}{23.6}\right)^3 + \left(\frac{(N_1)_{60cs}}{25.4}\right)^4 - 2.80 \quad (13)$$

$$MSF = 1 + (MSF_{max} - 1) \left(8.64 \exp\left(\frac{-M}{4}\right) - 1.325\right) \quad (14)$$

$$MSF_{max} = 1.09 + \left(\frac{(N_1)_{60cs}}{31.5}\right)^2 \leq 2.2 \quad (14)$$

$$K_\sigma = 1 - C_\sigma \ln\left(\frac{\sigma'_v}{P_a}\right) \leq 1.1 \quad (15)$$

$$C_\sigma = \frac{1}{18.9 - 2.55\sqrt{(N_1)_{60cs}}} \leq 0.3 \quad (16)$$

The CSR is equivalent to cyclic shear stress arising from earthquakes, calculated using Equation 17-20.

$$CSR_{M, \sigma'_v} = 0.65 \frac{\sigma'_v}{\sigma'_v} \frac{a_{max}}{g} r_d \quad (17)$$

$$r_d = \exp[\alpha(z) + \beta(z) \cdot M] \quad (18)$$

$$\alpha(z) = -1.012 - 1.126 \sin\left(\frac{z}{11.73} + 5.133\right) \quad (19)$$

$$\beta(z) = -0.106 - 0.118 \sin\left(\frac{z}{11.28} + 5.142\right) \quad (20)$$

In which σ'_v and σ'_v Are the total and the effective vertical pressures at a depth of z meters, $\frac{a_{max}}{g}$ represents the most significant horizontal acceleration due to earthquakes at ground level, r_d refers to decreased stress coefficient, P_a It is 101 kPa of overburden pressure. The liquefaction factor of safety value was subsequently employed to ascertain the soil lateral displacement index and reconsolidation settlement values in the study area.

2.2 Reconsolidation Settlement

The phenomenon of reconsolidation settlement on liquefaction pertains to soil subsidence after the dissipation of excess pore pressure caused by liquefaction, as observed during the reconsolidation process [15]. The settlement of the ground generated by liquefaction is directly related to the maximum shear strain experienced during undrained cyclic loading and the initial relative density of the sand [15]. The settling of sand layers can occur independent of the liquefaction of soil layers during motion. The reconsolidation settlement calculation utilizes the equation proposed by [6], which is expressed as 21-22.

$$\varepsilon_v = 1.5 \exp\left(-0.369\sqrt{(N_1)_{60cs}}\right) \cdot \min(0.08\gamma_{max}) \quad (21)$$

$$S_{v-1D} = \int_0^{z_{max}} \varepsilon_v dz \quad (22)$$

As ε_v represents the volumetric strain and S_{v-1D} is the ground's surface settlement for single-dimensional consolidation. The previously one-dimensional post-liquefaction reconsolidation settlement estimation depends on the liquefied zone's relative location and the evaluated structure type.

2.2.1 The ground settlement with damage severity

The examination of the relationship between estimated settlement and the amount of damage that occurs can be facilitated by employing various categories of [16] research. Table 1 presents data regarding the correlation.

Table 1. Settlements damage classification [16].

Settlements (cm)	Categories
0 – 10	Light to no damage
10 – 30	Moderate damage
30 – 70	Extensive damage

Various phenomena can be observed on the surfaces of the ground, categorized according to the severity of the damage. Minor cracks may occur for settlements ranging from 0 to 10 cm. The presence of minor fractures and sand oozing can be observed within the range of 10 to 30 centimeters of habitation. In addition, the settlement ranging from 30 to 70 cm potentially resulted in significant damage to the ground's surface, such as the formation of extensive fissures, the expulsion of sand, substantial displacement, and horizontal shifting [16].

2.3 Finite element geotechnical analysis

The application of Midas GTS NX software for conducting finite element geotechnical analysis is a widely adopted approach within the domain of geotechnical engineering. The Midas GTS NX software is a sophisticated finite element tool designed for simulating diverse geotechnical issues, including the significant deformations observed in underlying strata displacement resulting from mining subsidence or the construction of new surface buildings [17]. This method is commonly used to analyze the behavior of foundation systems, slope stability, soil-structure interaction, and seismic response. The data acquired from recent soil research conducted in 2021 is utilized as an input parameter within the Midas GTS NX software. Then, an analysis of potential soil displacement at the borehole site in the irrigation canal reconstruction project is performed.

3 Results and discussion

3.1 Potential Soil Displacement

The evaluation of probable soil displacement commences by determining the liquefaction safety factor inside the soil stratum. The Ministry of Public Works and Housing conducted soil investigations, obtaining data on the Standard Penetration Test (SPT) and bore log values for soil layers within a depth range of 15 to 20 meters. Furthermore, with the SPT data, Multichannel Analysis Surface Wave (MASW) data was acquired at two specific depths: 10 meters (VS10) and 30 meters (VS30).

Determining the soil layer's safety factor against liquefaction involves examining the groundwater level at the specific borehole location on November 30, 2021, denoted as the initial scenario. This study also implemented the second scenario with a groundwater level of -3.5 meters [3], while the third used a groundwater depth of -11 meters. Assessing soil displacement resulting from groundwater level changes

is crucial in understanding the phenomenon of liquefaction, as the groundwater level plays a significant role in initiating this process. The spatial distribution of the test points within the Jono oge and Lolu regions is depicted in Figure 3.

The preceding investigation has acquired the FS_{Liq} values for every soil layer within the reconstruction area [7]. Two boreholes exist, namely BH6 and BH9, which are situated beyond the confines of the principal irrigation canal's site. The purpose of doing SPT tests was to see if there were any notable variations in soil characteristics between the principal canal and its surrounding areas.

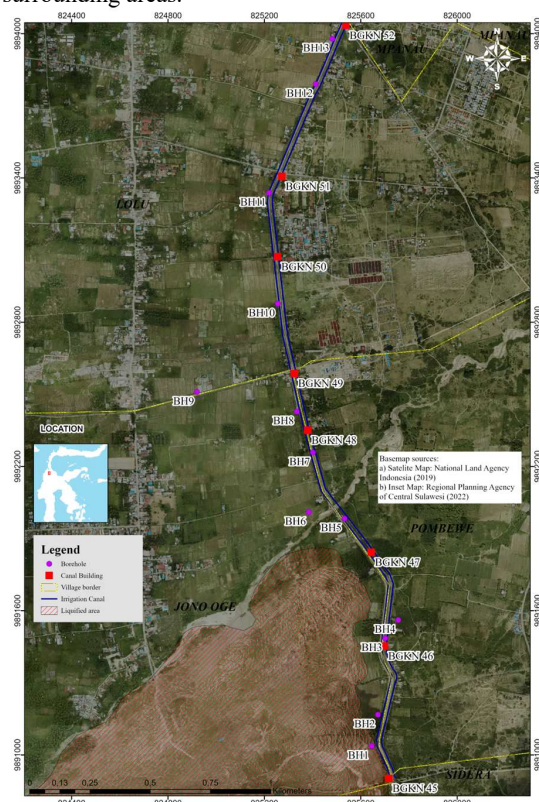


Fig. 3. The borehole and canal building location in Jono Oge and Lolu area (modified from [18]).

According to the previous findings, the liquefaction safety factor indicates that within the soil depth range of 5.5 meters to 18 meters are prone to re-liquefaction, as indicated by the $FS_{Liq} < 1$ value, across three distinct scenarios [7]. The findings presented in this study demonstrate similarities with other research, which has indicated a somewhat elevated liquefaction potential in the research location [3,19,20]. In addition, an assessment was conducted to determine the potential for soil displacement, specifically in terms of lateral displacement index and reconsolidation settlement. The findings of this assessment are elaborated upon in the subsequent sections.

3.1.1 Soil lateral displacement index results

The analysis of the lateral displacement index is conducted by equation 1. The outcomes of the LDI

metric are observable in Table 2. This soil displacement may manifest if the earthquake exhibits a magnitude equivalent to the 2018 calamity.

According to the LDI data presented in Table 2, the reconstruction sites located at BH2 and BH13 have the most significant possible soil lateral displacement value of 3.19 meters at the groundwater level conditions seen on November 30, 2021. There are a total of six places that exhibit an LDI value of zero. The reason for the lack of water in boreholes BH3, BH4, BH6, BH7, and BH12 is due to their dry condition [7]. Regarding the geographical coordinates of BH-10, it is noteworthy that the groundwater level in this area has a depth of around 10.38 meters. However, it is essential to highlight that the corresponding LDI value is recorded as 0. This phenomenon is because the average SPT value recorded at each depth exceeds 40. The LDI values were calculated for both Scenario 2 and Scenario 3. The findings are displayed in Table 3.

Table 2. LDI results in scenario one.

Borehole Name	Northing	Easting	GWL (m)	LDI (m)
BH1	9891037.093	825645.692	11.69	1.74
BH2	9891167.597	825671.262	4.00	3.19
BH3	9891485.645	825701.159	Dry	0.00
BH4	9891561.231	825755.958	Dry	0.00
BH5	9891983.377	825532.588	8.6	0.20
BH6	9892009.853	825384.094	Dry	0.00
BH7	9892258.052	825401.423	Dry	0.00
BH8	9892428.330	825334.498	7.49	2.33
BH9	9892509.692	824919.777	6.73	0.10
BH10	9892876.772	825255.526	10.38	0.00
BH11	9893337.574	825219.362	10.76	1.42
BH12	9893790.186	825413.363	Dry	0.00
BH13	9893978.766	825481.782	7.12	3.19

Table 3. LDI results on scenario two and scenario three.

Borehole Name	Scenario 2		Scenario 3	
	GWL (m)	LDI (m)	GWL (m)	LDI (m)
BH1	3.50	4.22	11.00	1.74
BH2	3.50	3.12	11.00	2.02
BH3	3.50	3.86	11.00	1.85
BH4	3.50	3.42	11.00	0.92
BH5	3.50	0.65	11.00	0.04
BH6	3.50	0.83	11.00	0.52
BH7	3.50	4.28	11.00	2.13
BH8	3.50	3.25	11.00	1.00
BH9	3.50	0.13	11.00	0.09
BH10	3.50	0.00	11.00	0.00
BH11	3.50	2.20	11.00	1.42
BH12	3.50	2.65	11.00	1.59
BH13	3.50	4.61	11.00	2.12

Following the second scenario, whereby the groundwater level is presumed to rise to a depth of -3.5 meters, it is observed that the BH7 region exhibits the most potential for soil lateral displacement in the irrigation canals within the Jono Oge area. Conversely, the BH9 location has the lowest magnitude of lateral displacement. Concerning the Lolu village region, it is observed that the highest LDI value is recorded at point BH13, measuring 4.61 meters. Conversely, the lowest

LDI value is documented at point BH10, with a measurement of 0. Scenario 3 shows a similar tendency in the soil lateral displacement index value. This value of LDI is reduced due to the implementation of groundwater level control measures, which aim to maintain the groundwater level at -11 meters below ground level along the site of irrigation canal reconstruction.

3.1.2 Reconsolidation settlement results

The determination of the reconsolidation settlement value outcomes in the subsequent section is predicated upon the utilization of Equation 21. The potential for damage caused by settlements in the Jono Oge and Lolu area relies upon the groundwater level. If the groundwater level remains unchanged, as known on November 30, 2021, the BH2 location has a 0.34 m settlement, and substantial damage may occur. The possible impact resulting from the land settlement in the Lolu region resembles that observed in the village of Jono Oge. The most notable soil settlement will occur at the BH13 site, with a value of 0.32 meters if re-liquefaction is triggered. Table 4 presents an overview of the Potential Reconsolidation Settlement Value for Scenario 1.

Table 4. Soil settlement results in scenario one.

Borehole Name	S (m)	Categories
BH1	0.15	Moderate damage
BH2	0.34	Extensive damage
BH3	0.00	Light to no damage
BH4	0.00	Light to no damage
BH5	0.05	Light to no damage
BH6	0.00	Light to no damage
BH7	0.00	Light to no damage
BH8	0.21	Moderate damage
BH9	0.02	Light to no damage
BH10	0.00	Light to no damage
BH11	0.16	Moderate damage
BH12	0.00	Light to no damage
BH13	0.32	Extensive damage

Table 5 displays the results of the soil reconsolidation settlement in the second and third scenarios. According to the data presented in Table 5, it can be observed that there is an elevation in the groundwater level in all borehole locations in scenario 2. This rise in groundwater level leads to the saturation of the soil layer with water. Consequently, the likelihood of ground settlement is heightened in scenario 2, mainly if liquefaction occurs. The BH7 point, previously deemed, underwent a substantial settling of 0.41 meters under the category of extensive damage. In the Lolu area, it is worth noting that the primary irrigation canal also exhibits the possibility of settlement at Location BH13, with a potential subsidence of 0.44 meters. In the third scenario, wherein the groundwater level is uniformly lowered to -11 meters, the reconstruction site does not undergo significant damage in the event of an earthquake capable of inducing liquefaction.

Table 5. Soil settlement results in scenario two and scenario three.

Borehole Name	Scenario 2		Scenario 3	
	S (m)	Categories	S (m)	Categories
BH1	0.39	Extensive damage	0.15	Moderate damage
BH2	0.34	Extensive damage	0.19	Moderate damage
BH3	0.38	Extensive damage	0.19	Moderate damage
BH4	0.35	Extensive damage	0.11	Moderate damage
BH5	0.10	Light to no damage	0.01	Light to no damage
BH6	0.13	Moderate damage	0.08	Light to no damage
BH7	0.41	Extensive damage	0.22	Moderate damage
BH8	0.30	Extensive damage	0.10	Moderate damage
BH9	0.03	Light to no damage	0.02	Light to no damage
BH10	0.00	Light to no damage	0.00	Light to no damage
BH11	0.25	Moderate damage	0.16	Moderate damage
BH12	0.31	Extensive damage	0.20	Moderate damage
BH13	0.44	Extensive damage	0.20	Moderate damage

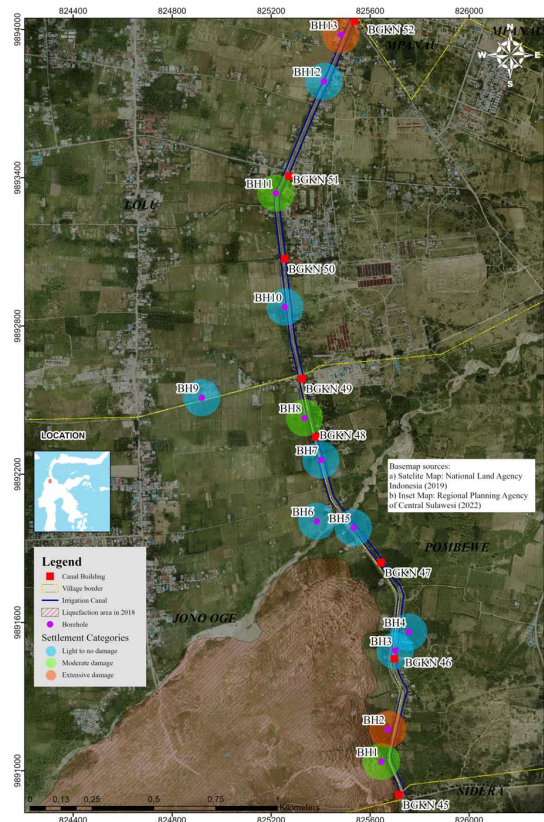


Fig. 4. Mapping of reconsolidation settlement in Jono Oge and Lolu areas at GWL November 30, 2021 (modified from [18]).

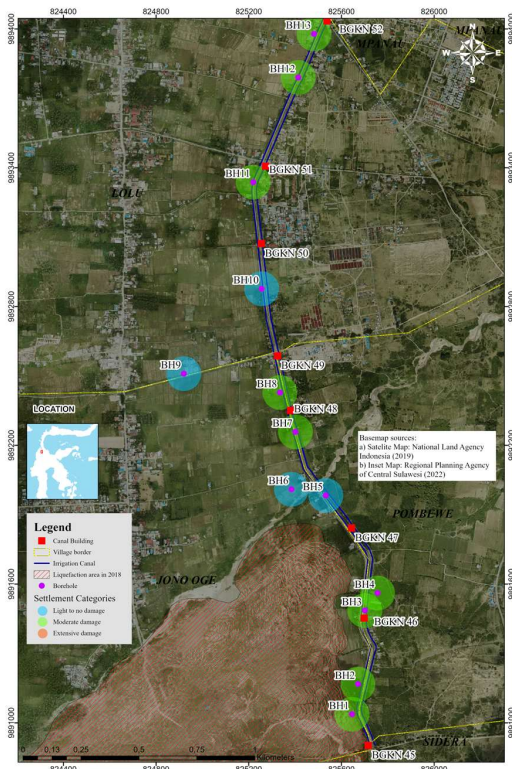


Fig. 5. Mapping of reconsolidation settlement in Jono Oge and Lolu areas in the third scenario (modified from [18]).

In addition, the potential damage categories resulting from settlement in Scenario 1 and Scenario 3 are delineated along the research location, as depicted in Figure 4 and Figure 5. According to the mapping data, it is indicated that segments BGKN 45 - BGKN 46, as well as BGKN 52, have the potential to undergo significant damage as a result of settlement. Suppose the groundwater level can be effectively regulated, as depicted in scenario 3. In that case, it can be inferred from Figure 5 that the occurrence of substantial damage in subsequent reconstruction segments will be mitigated.

3.1.3 Finite element analysis results

The finite element analysis and modeling using the Midas GTS NX program were conducted to investigate the possible soil layer displacement during liquefaction. A dynamic analysis was performed to assess the potential of horizontal displacement (TX Translation) that may occur under the influence of earthquake loads. One of the aspects examined in this study pertains to BH1, which is modeled under the groundwater level scenarios of -11.69 meters and -3.5 meters. The borehole 1 location is close to the flow-slide liquefaction site in the Jono Oge area. The analysis employed a two-dimensional (2D) plain strain methodology, incorporating soil input parameters like elastic modulus (E), Poisson's ratio (ν), soil unit weight (γ), cohesion (C), and frictional angle (Φ). The input parameters are outlined in Table 6.

The soil layer in Figure 6 is represented by a model that extends to a depth of 15 meters and has a width of 58 meters. The soil boundary condition is implemented by utilizing the auto constraint menu within the Midas-GTS NX software. Without dynamic forces, the displacement resulting from the gravitational load (self-weight) is measured to be zero (0) when the option to clear the initial displacement menu in the analysis settings is activated.

The construction stage analysis in Midas GTS-NX involves initial and dynamic conditions considering the model self-weight. The dynamic analysis employed the historical data from the Kobe 1995 earthquake with a magnitude of 6.9 Mw [21]. The geometric configuration entered into the model may be shown in Figure 6. The results of soil layer deformation under dynamic conditions under different groundwater levels are presented in Figure 7 and Figure 8, respectively.

Table 6. Input parameters on soil modeling.

Name	Sand 1	Sand 2	Sand 3
Material	Isotropic	Isotropic	Isotropic
Model Type	Mohr-Coulomb	Mohr-Coulomb	Mohr-Coulomb
Elastic Modulus (E) (kN/M ²)	50.000	50.000	50.000
Poisson's Ratio (ν)	0.30	0.30	0.30
Unit Weight (γ) (kN/M ³)	16.00	17.00	18.00
Ko	Auto	Auto	Auto
Saturated Unit Weight (kN/M ³)	17.00	18.00	20.00
Drainage Parameter	Drained	Drained	Drained
Cohesion (C) (kN/m ²)	1.00	1.00	1.00
Frictional Angel (Φ) (deg)	23.80	32.00	34.00
Depth (m)	1 – 4.95	4.95 – 10.5	10.5 – 15

The dynamic analysis results for groundwater levels of 14.69 meters and -3.5 meters are depicted in Figure 7 and Figure 8, respectively. The soil layer was exposed to an earthquake load using a Time History Load Function. The load was based on recorded data from the 1995 Kobe earthquake, which lasted 50 seconds and had an acceleration value of -0.5685g. The investigation revealed that the dynamic load induced a maximum horizontal displacement of 1.77 meters when the groundwater level was -11.69 meters. When the groundwater table is raised to -3.5 meters, the horizontal displacement also increases to a maximum of 3.76 meters. The horizontal displacement value obtained in the finite element analysis closely approximates the semi-empirical analysis at BH1 in the first and second scenarios, as outlined in Table 3. The reconstruction process for irrigation canals in the study area necessitates careful consideration of the potential soil lateral displacement magnitude that may

arise due to the groundwater levels.

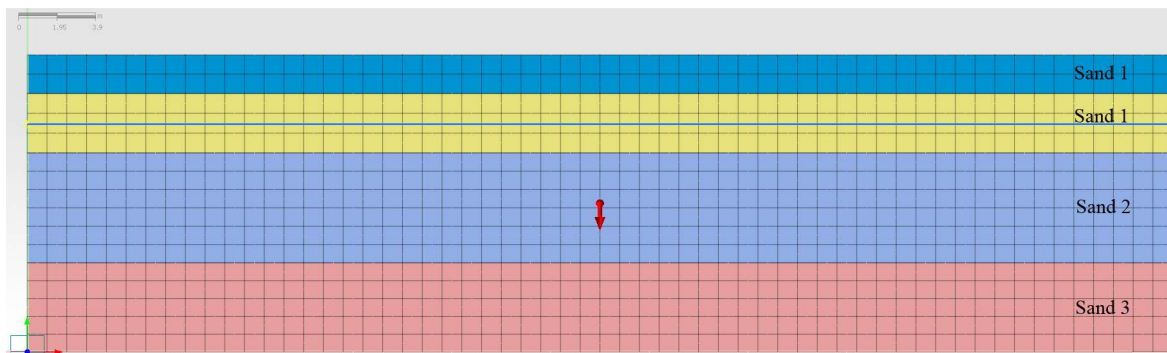


Fig. 6. Finite element modeling of soil layers, loading, and meshing on BH1.

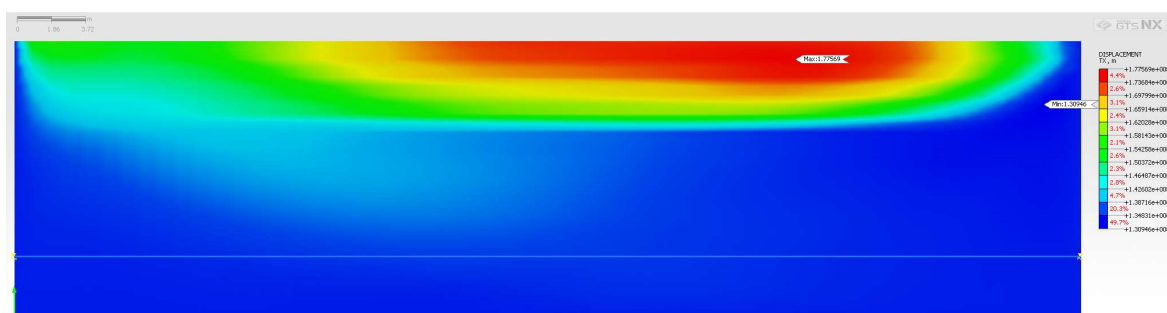


Fig. 7. The horizontal displacement results (TX Translation) of finite element modeling on BH1 with scenario 1.

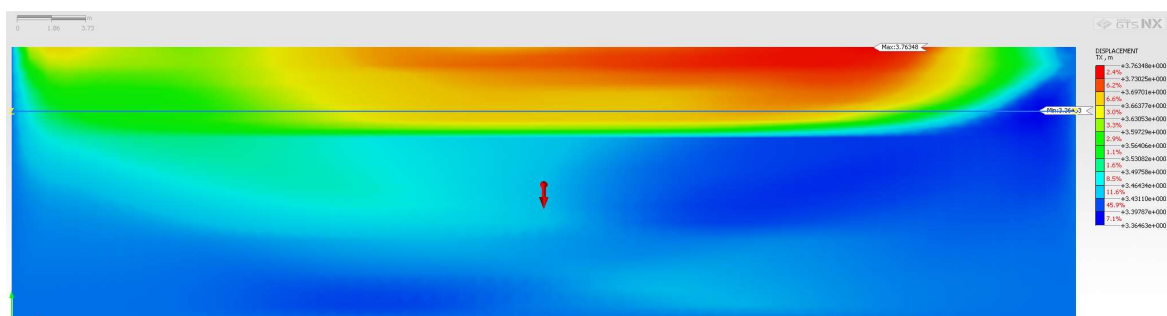


Fig. 8 The horizontal displacement results (TX Translation) of finite element modeling on BH1 with scenario 2.

The Ministry of Public Works and Housing already plans several mitigation strategies. Various approaches can be employed to mitigate liquefaction, including soil compaction, groundwater level management, and engineering measures for irrigation canal infrastructure. One of these involves the implementation of geomembranes to line irrigation canals intending to prevent water seepage. In order to mitigate the risk of infrastructure damage caused by liquefaction, there is an ongoing effort to create stone-filled trenches along the segment with the high re-liquefaction potential of the irrigation canals in Jono Oge [7]. Additionally, there are proposed initiatives to develop monitoring wells and groundwater pumping to mitigate excess pore pressure in the region during an earthquake.

4 Conclusion

The soil investigation reveals that the irrigation canals in Jono Oge and Lolu area predominantly consist of sandy soil. The groundwater table in the specified region has relatively shallow depths, ranging from -4m to -11.69m below the ground surface. This characteristic suggests the potential for liquefaction to reoccur in the study location's primary canals.

According to the analysis of the most recent recorded groundwater level, the lateral displacement index study outcomes indicate that BH2 and BH13 exhibit the highest propensity for lateral ground displacement, surpassing a magnitude of 3 meters. The findings of the reconsolidation settlement analysis likewise demonstrate comparable outcomes above a threshold of 30cm, hence signifying substantial damage to both the soil and structures. Furthermore, the findings from the analysis of ground displacement, considering

different groundwater level scenarios, indicate that variations in groundwater levels significantly impact the extent of ground displacement.

In order to mitigate the lateral displacement and land subsidence resulting from liquefaction, it is advisable to regulate the groundwater level at the site of the primary irrigation canal. Routine monitoring of groundwater levels through establishing monitoring wells at the sites of irrigation canals and groundwater pumping in the Jono Oge and Lolu regions can effectively contribute to reducing groundwater levels in the event of a rise. In subsequent investigations, the anticipated extent of soil displacement will be compared with the outcomes of simulating the implementation of liquefaction mitigation techniques at the site of the irrigation canal.

The authors express their gratitude for the support provided by the River Basin Organization Sulawesi III Palu, the Directorate General of Water Resources, and Midas Indonesia.

References

1. H. Hazarika, D. Rohit, S. M. K. Pasha, T. Maeda, I. Masyhur, A. Arsyad, S. Nurdin, *Soils Found.* **61**, 1 (2021)
2. T. Kiyota, H. Furuichi, R. F. Hidayat, N. Tada, H. Nawir, *Soils Found.* **60**, 3 (2020)
3. A. Pratama, T. F. Fathani, and I. Satyarno, *Liquefaction potential analysis on Gumbasa Irrigation Area in Central Sulawesi Province after 2018 earthquake*, in IOP Conference Series: Earth and Environmental Science (2021)
4. A. Widyatmoko, D. Legono, and H. C. Hardiyatmo, *Potential Study of Liquefaction in the Downstream Area of Jono Oge-Paneki River, Central Sulawesi*, in IOP Conference Series: Earth and Environmental Science (2021)
5. G. Zhang, P. K. Robertson, R. W. I. Brachman, *J Geotech Geoenviron* **130**, 8 (2004)
6. M. Yoshimine, H. Nishizaki, K. Amano, Y. Hosono, *Soil Dyn. Earthq. Eng.* **26**, 2-4 (2006)
7. I. M. Widyana, S. Ismanti, and A. F. Setiawan, *Liquefaction potential evaluation on reconstruction project of irrigation canal in the Jono Oge and Lolu Village* in E3S Web Conf. 429, 04012 (2023)
8. L. Z. Mase, *Media Komunikasi Teknik Sipil* **27**, 1 (2021)
9. C. Suhartini, L. Z. Mase, and M. S. Farid, *Mapping the Liquefaction Potential Index (LPI) in Ratu Agung Subdistrict, Bengkulu City, Indonesia Using the Shear Wave Velocity Approach* in E3S Web of Conferences (2021)
10. S. G. Manoharan and G. P. Ganapathy, *Geoenvironmental Disasters* **10**, (2023)
11. A. N. Andiny, F. Faris, and A. D. Adi, *Slope Stability Analysis During an Earthquake in Flow-Slide Affected Area of Jono Oge*, in IOP Conference Series: Earth and Environmental Science (2022)
12. A. Jalil, T. F. Fathani, I. Satyarno, W. Wilopo, *Geoenvironmental Disasters* (2021)
13. D. Zheng, L. L. Tang, Y. Wang, Y. Chen, *Advances in Civil Engineering* (2022)
14. R. W. Boulanger and I. M. Idriss, *CPT And SPT Based Liquefaction Triggering Procedures*, in Report No. UCD/CGM-14/01 Department Of Civil & Environmental Engineering College Of Engineering University Of California (2014)
15. F. Nurdiansyah, A. D. Adi, and S. Ismanti, *Settlement Analysis in Potentially Liquefiable Soil at Kretek 2 Bridge Area*, IOP Conference Series Earth and Environmental Science (2023)
16. K. Ishihara, *Soil Behaviour in Earthquake Geotechnics* (Clarendon Press, Oxford University Press, 1996)
17. X. Zhang, W. Li, T. Li, Z. Li, G. Cai, Z. Shen, R. Li, *Front Earth Sci.* **11**, (2023)
18. National Land Agency Indonesia, *Citra PASIGALA Tahun 2019*, in Pasigala Image Documentation (2019)
19. A. N. Andiny, F. Faris, and A. D. Adi, *Re-liquefaction hazard evaluation in flow-slide affected area of Jono Oge, Central Sulawesi, Indonesia*, in IOP Conference Series: Earth and Environmental Science (2021)
20. W. Rahayu, Nurizkatilah, and E. Bahsan, *Analysis of liquefaction potential in Lolu Village, Palu using SPT method and laboratory test of grain size distribution*, in IOP Conference Series: Earth and Environmental Science (2021)
21. A. Jalil, T. F. Fathani, I. Satyarno, and W. Wilopo, *Nonlinear site response analysis approach to investigate the effect of pore water pressure on liquefaction in Palu*, in IOP Conf. Ser.: Earth Environ. Sci. 871, 012053 (2021)